Proc. Natl. Acad. Sci. USA
Vol. 96, pp. 4228–4231, April 1999

Perspective

Real or virtual large-scale structure?

August E. Evrard

Physics Department, University of Michigan, Ann Arbor, MI 48109-1120

Modeling the development of structure in the universe on galactic and larger scales is the challenge that drives the field of computational cosmology. Here, photorealism is used as a simple, yet expert, means of assessing the degree to which virtual worlds succeed in replicating our own.

Our current cosmic environment is awash with diverse, complex structures—black holes, starburst galaxies, superclusters—which span a tremendous range of physical scales and incorporate a remarkable variety of physical conditions. Yet, a few hundred thousand years after the Big Bang, the terrain of the universe was nearly featureless. As revealed by NASA's COBE satellite, the lukewarm matter and radiation fields back then were exquisitely uniform, with conditions from one location in space to the next varying by only a few parts in 10^5. To understand this remarkable transition—from the simple to the sublime—is a fundamental quest of modern cosmology.

In the search for answers, numerical simulation of cosmic structure, a field known as "computational cosmology" (1), plays a critical role. The formal complexity of the physical problem—to solve for the fully three-dimensional evolution of a set of coupled fluids (dark matter, baryonic matter, stars, and radiation) from a linear, initial state into the deeply nonlinear regime—means that direct numerical solution of the governing equations is, with rare exception, the only viable approach. As an enterprise, computational cosmology straddles the traditional domains of theory and experiment. Functioning as theorists, simulators gain physical insight by examining the dynamical behavior of idealized cosmic systems. Such systems, necessarily incomplete by their discrete, finite nature, grow closer to their true astronomical counterparts as the input physics and numerical resolution improve. This leads to the ultimate role of the simulator as experimentalist. Creating other universes in the terrestrial laboratory is impossible, but tinkering with "virtual worlds" inside a computer is not.

As a means for conveying an impression of the current state of affairs in computational cosmology, I have chosen a theme reminiscent of the old Memorex tape ads: "Is it real or is it virtual?" Four topics are highlighted, and for each a figure is provided, juxtaposing real observations with data from the virtual realm. The status of our understanding is reflected by the degree of correspondence within each pair of images. Of course, the purpose of these images is not just to make pretty pictures. Synthetic observations help quantify errors associated with working with data projected on the sky and comparison between real and synthetic observations provides critical assessment of cosmological models. A few of the lessons learned from simulations are highlighted in the examples below.

Preliminaries

The favored theoretical framework for the emergence of structure in the universe marries the traditional hot, Big Bang cosmology with a very early epoch of rapid expansion of space known as inflation (2). The simplest flavors of such models now possess 15 or so adjustable parameters, only one of which (the energy density in photons) is incontestably determined to better than 10% precision. Hubble's constant H_0, which relates recession velocity to distance locally, sets the present critical mass density of the universe $\rho_c \equiv H_0^2/8\pi G$, which is used to express component densities in dimensionless form $\Omega_X = \rho_x/\rho_c$. The mix of components {X} includes ordinary (baryonic) matter Ω_b, cold dark matter Ω_{cdm}, hot dark matter Ω_{hdm}, and vacuum energy (formerly known as the cosmological constant) Ω_L. A convenient measure is the total matter content $\Omega_m = \Omega_b + \Omega_{cdm} + \Omega_{hdm}$.

Minimally baroque models of inflation predict a flat space-time metric, which constrains the total energy density $\Omega_m + \Omega_\Lambda = 1$. More importantly, inflation provides a mechanism for introducing fluctuations into the energy density, thus seeding structure formation. The fluctuations have the character of a Gaussian random process uniquely specified by the mean square amplitude of fluctuations as a function of wavenumber k (related to wavelength λ by $k = 2\pi/\lambda$), the primordial power spectrum $P_{prim}(k)$. Theory predicts a power-law spectrum fluctuations with slope close to unity, and the normalizing amplitude is a free parameter to be fit empirically. COBE observations indicate a characteristic fractional amplitude that is very small, $\delta\rho/\rho \approx 10^{-5}$ (3). Physics operating during the "middle ages" of the universe (from 1 s up to 100,000 years, when the radiation field cools sufficiently to allow neutral H/He in abundance and the universe becomes transparent to radiation) modifies the fluctuations in ways that depend on the entire cosmic mix of components. Because the fluctuation amplitudes are small, a linear treatment of individual modes (each being a single wavenumber, k) provides an accurate treatment of the physical processes, and the net effect is summarized in a single transfer function $T(k)$. The result is a "processed" power spectrum of density fluctuations, $P(k) = T(k)\,P_{prim}(k)$, which is used as the starting point for simulations.

The general aim of a simulation is to evolve a finite realization of a particular cosmological model forward in time from its linear, initial state to a later, nonlinear regime. Technical details of simulations vary from one research group to the next, but all methods have in common a choice of spatial discretization scheme and a method for integrating the equations of motion forward in time. Memory usage, speed, stability, and accuracy all are considerations in algorithm design and code implementation. A summary of 12 different cosmological codes and a comparison of their output when applied to a fixed problem of forming a large galaxy cluster provides a reference point for those interested in technical details (4).

Because gravity acts on all components and on all scales, it is the central physical element incorporated. A variety of tricks are used to speed the solution of Poisson's equation, including use of fast Fourier transforms (FFTs), FFTs with small-scale spatial corrections, and hierarchical tree methods. What additional physics beyond gravity is incorporated varies depending on the problem at hand.

Zeroing in on the parameter set of our universe is a perennial quest for cosmologists, and a preferred region of parameter space naturally exists at any time. In the decade from the mid-1980s to mid-90s, models with high mass density $\Omega_m = 1$ and zero cosmological constant held the high ground. Mounting evidence

PNAS is available online at www.pnas.org.

for a low total mass density and a possible nonzero vacuum energy density (28) has turned the spotlight to vacuum energy-dominated models with $\Omega_m \simeq 0.3$ and $\Omega_\Lambda \simeq 0.7$. The examples below are drawn from simulations of these two classes of models.

The Cosmic Web of Galaxies and Dark Matter

Early estimates of galaxy counts on the sky from photographic plates showed that their spatial arrangement was inconsistent with a Poisson random distribution (5). The three-dimensional morphology of the clustering pattern of galaxies emerged with redshift surveys covering large areas of the sky (6). Descriptive terminology erupted in the literature—bubbles, pancakes, walls, voids, superclusters, and so on—and questions arose as to whether gravitational instability of a Gaussian noise field could produce such a variety of morphological features.

Fig. 1 provides an answer in the affirmative. One panel shows positions in "redshift space" for roughly 25,000 galaxies in the ongoing two-degree field (2dF) survey (http://msowww.anu.edu.au/~colless/2dF/). The other shows a mock galaxy catalogue generated from an $\Omega_m = 1$ CDM (cold dark matter) universe simulation (7). A galaxy luminosity function and 2dF magnitude selection limit have been imposed on the simulation map, and this produces a decline in the number of pseudo-galaxies with distance similar to that of the observed catalogue. Which map is which? Both display a similar texture: a surrounding web-like network (8) defines nearly empty voids, with rich clusters formed at the intersection of filaments in the web. The features aren't perfectly sharp in either map. This fractal characteristic reflects gravity's lack of scale and the incoherence of the initial density field.

A variety of statistics verify that the texture of the large-scale web of galaxies is consistent with gravitational amplification of initially small, Gaussian perturbations. That's the good news. What's the bad? Detailed constraints on cosmological models are difficult to place from these data alone. The reason is that simulations of large volumes model only the dominant dark matter component, while observational catalogues map visible galaxies. How well galaxies trace the dark matter is an unresolved issue, but the correspondence is not likely to be simple. Catalogues of different types of galaxies (ellipticals versus spirals, infrared versus optically selected) exhibit clustering properties that differ with respect to each other (9). What class, if any, traces exactly the underlying dark matter?

The suspicion of a biased galaxy population is strengthened by consideration of the shape of the spatial auto-correlation function $\xi(r)$, the Fourier transform of the evolved power spectrum, $P(k)$. For optically selected galaxies, this function is observed to be extremely close to a power law $\xi(r) \propto r^{-1.8}$ over almost three decades in length scale. Analysis of some of the largest dark matter simulations to date (10) finds that none of the popular models produce dark matter autocorrelation shapes consistent with the galaxy observations over all scales, implying a scale-dependent bias of galaxies relative to dark matter. In the coming era of very large redshift surveys such as the 2dF and the Sloan Digital Sky Survey (http://www.sdss.org/), we stand to learn as much about the astrophysics of galaxy formation as we do about our underlying cosmology.

A Filamentary Forest

Viable cosmological models form structure in a hierarchical fashion over time. The web-like network, evident on large spatial scales in Fig. 1, initially emerges on a much smaller spatial scale at high redshift. Galaxies and quasars (quasi-stellar objects, QSOs), which are observed up to redshifts of 5, are believed to form at the knots of the filamentary web (29). As continuum radiation from distant, bright QSOs passes through the intervening, evolving web of baryonic matter and dark matter, any neutral hydrogen (HI) encountered at redshifts z along the way will readily scatter photons with wavelengths at the Lyman-α transition in the HI rest frame 1216 (1+z) Å (11). Since the HI density is higher in the knots and filaments and lower in the intervening voids, photons that happen to be crossing a void while redshifting through 1,216 Å pass to us unhindered, while those that do so while crossing a filament will have a finite probability of being scattered out of our line of sight. As a result, the QSO spectrum received at Earth is imprinted with a "forest" of absorption troughs, shadows of the distribution of matter lying between us and the distant quasar.

Fig. 2 exhibits real and virtual examples of Lyman-α forest absorption spectra. Their character is strikingly similar. The simulated spectrum is generated from the solution for the baryon plasma's density and temperature, with an added assumption for the intensity Γ_{HI} of the metagalactic ionizing radiation field. The value of Γ_{HI} is set by matching the mean optical depth $\bar{\tau}$ of the observed spectrum, meaning that the integrals of the two spectra of Fig. 2 match. But the nature of the excursions beneath the continuum level is determined by the spatial structure within the simulation. As emphasized by the first simulations of this type (12–14), the similarity of the two spectra supports a cosmic web interpretation for the origin of forest lines and effectively lays to rest prior models for the Lyman-α forest based on intergalactic, pressure-confined clouds.

The mean optical depth constraint provides a useful lower bound on the baryon density parameter Ω_b. The argument uses the fact that $\bar{\tau}$ depends on the baryon density parameter and ionizing flux through $\bar{\tau} \propto \Omega_b^2/\Gamma_{HI}$.

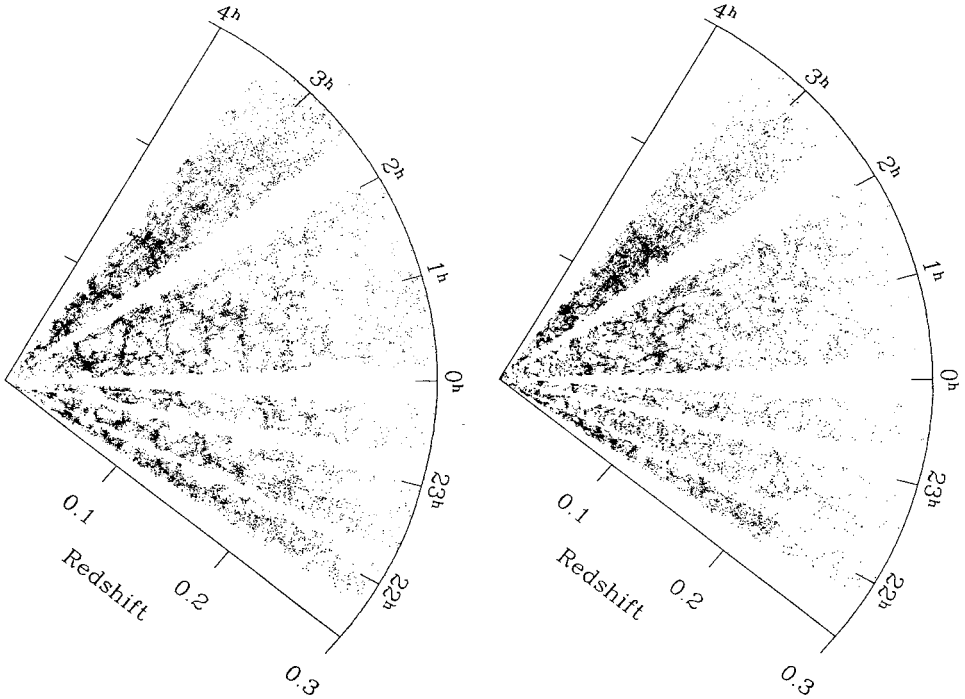

FIG. 1. Galaxies in the 2dF survey paired against a biased selection of cold dark matter particles drawn from an $\Omega_m = 1$ simulation. Figure courtesy of P. Norberg, S. Cole, and the 2dF collaboration.

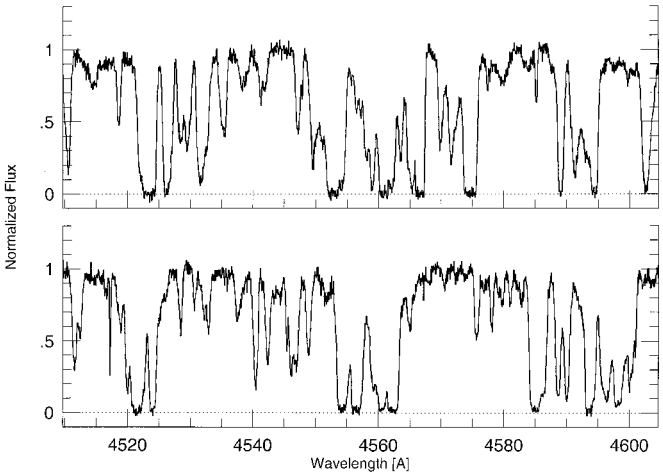

FIG. 2. Absorption line spectrum from a Keck telescope observation of a QSO at redshift $z = 3.62$ twinned with a synthetic spectra generated by using the neutral hydrogen distribution from a simulation of a universe dominated by vacuum energy. Figure courtesy of R. Dave and D. Weinberg. The Keck spectrum is reprinted from ref. 15 with permission.

Counts of high redshift QSOs can be used to impose a minimum value for the ionizing background, and this in turn bounds Ω_b from below. Essentially, a very low-density universe would be very highly ionized and exhibit no detectable absorption features. The bounds obtained from this method are very close to the current best estimate value $\Omega_b\, h_2 = 0.019 \pm 0.001$ (where $h = H_o/100$ km s^{-1}·Mpc^{-1}) recently obtained from comparison of nucleosynthesis predictions with the deuterium abundance derived from high signal-to-noise spectra of QSOs (16, 17). This indicates that most of the baryons in the universe at $z \simeq 2$–3 are associated with the absorbing cosmic web; only a small mass fraction would be incorporated into galaxies at that time (29). The situation is thought to be similar today, except that the characteristic scale of the web is larger, and the baryons reside in a comparatively warmer ($\simeq 10^5$ K) intergalactic medium (18).

The radiation spectrum carries with it statistical information about the total underlying mass density along the line of sight back to the QSO. Because the physical conditions within the low-density features that generate the bulk of the scattering cross-section are relatively simple, an analytic link between HI optical depth and total mass density can be made reliably (19, 20). This allows, for the first time, a robust estimate of the linear-regime mass power spectrum directly from the one-dimensional optical depth power spectrum of the data in Fig. 2. The first attempt of this measurement confirms the power spectrum shape predicted by inflation models with mass content dominated by cold, dark matter (21).

X-Ray Behemoths

Rich clusters of galaxies are the blue whales of the cosmos; they are the largest equilibrated structures in the universe. Fed a regular diet of mergers with less massive galactic groups over the gigayears, the largest today contain several thousand galaxies as massive as our Milky Way. First identified optically as regions of enhanced galaxy density, it was the revelation by Zwicky in 1933 (22) that the gravitational binding mass of the Coma cluster far exceeded that associated with the visible light in the galaxies that demonstrated the need for universal dark matter. In the past two decades, imaging by x-ray satellites has revealed huge amounts of hot (10^7–10^8 K) plasma filling the space between the galaxies in clusters. In the biggest clusters, the mass associated with this intracluster medium (ICM) is larger by a factor of 10 than the mass associated with the galaxies, making the ICM the dominant baryonic component, second overall to the dark matter.

Because galaxies are such a minority player in the biggest clusters, first attempts at simulating the multicomponent properties of clusters ignored them altogether (23). In such models, the collisionless dark matter is gravitationally coupled to a collisional baryon gas that is subject to merger-induced shock heating and support from thermal pressure with an ideal gas equation of state. The massive potential wells attain temperatures up to 10^8 K, and the highly ionized ICM plasma liberally emits x-rays via thermal bremsstrahlung (electron-ion scattering). Fig. 3 displays a characteristic x-ray image of such a simulation, paired with an image of the modest cluster AWM7 from the ROSAT archives (24). The synthetic image was generated by sampling a total of 10,000 photons in the 0.5–2.0 keV ROSAT energy band, appropriate to match the moderate resolution image of AWM7. Both objects display regular, slightly elliptical isophotes (contours of constant brightness). In the simulation, this structure results from the ICM being very close to hydrostatic equilibrium within an ellipsoidal potential well dominated by cold, dark matter.

Considered as a family, both observed and simulated x-ray clusters display a remarkable degree of regularity. The total luminosities (after removal of cooling flow cores) and isophotal sizes of clusters correlate tightly with x-ray temperature. The data limit variations in ICM gas mass fraction to be small, typically $\lesssim 13\%$ (25, 26). Virtual clusters are even more regular; their local baryon mass fractions display $\approx 5\%$ scatter about a value approximately 10% lower than the universal fraction Ω_b/Ω_m. The mix of baryons and dark matter in rich clusters thus provides a clean and relatively unbiased view of the cosmic mix. Coupling measured ICM mass fractions with limits on the baryon density derived from the primordial deuterium abundance (17) results in a stringent constraint on the mass density parameter, $\Omega_m\, h^{2/3} = 0.30 \pm 0.07$ (27). This line of argument is one of the strongest pieces of evidence against a universe with critical mass density ($\Omega_m = 1$).

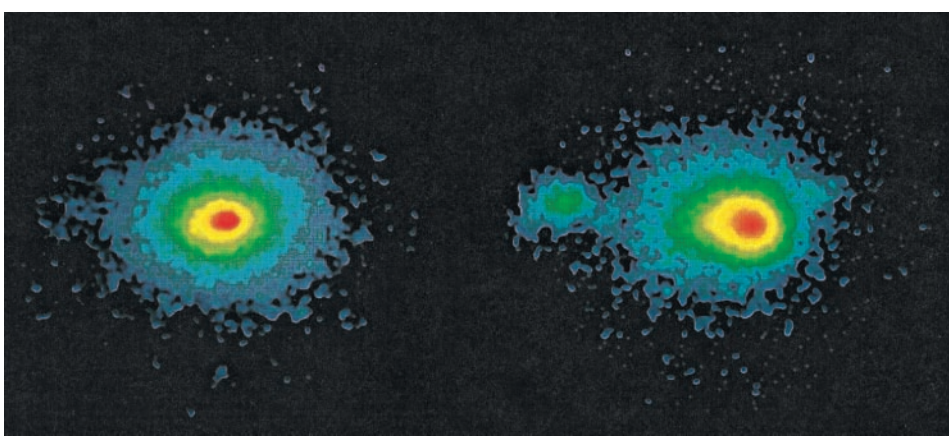

FIG. 3. Maps of the 0.1–2.4 keV x-ray emission from the cluster of galaxies AWM7 along with emission from a cluster simulated within a universe dominated by vacuum energy density. The linear scale of each image is ≈ 3 Mpc. Observational image courtesy of J. Mohr and B. Mathiesen.

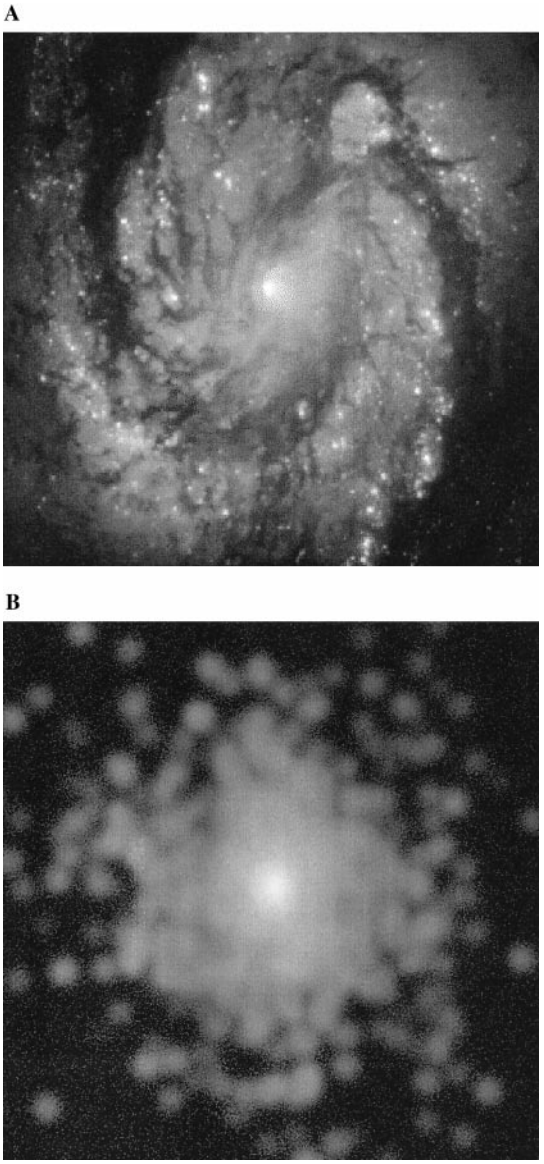

FIG. 4. An HST WFPC-2 image of the local spiral galaxy M100 along with stellar emission from a simulated disk galaxy synthetically imaged in the HST I-band. Observational image courtesy of NASA, simulated image courtesy of M. Steinmetz.

The Final Frontier

The relative simplicity of the gas dynamics in the Lyman-α forest and intracluster medium applications has made possible the rapid advances in understanding of those systems. The problem of galaxy formation poses a more formidable challenge to computational cosmology. Star formation and the interplay between stars and the surrounding interstellar medium introduce large modeling uncertainties into present calculations and pose formidable obstacles to future progress. In some sufficiently small patch of a galaxy, magnetic fields, radiation transfer, and local composition can affect, and perhaps in turns dominate, the local gas dynamics and thermodynamics. Yet there have been few serious attempts to model these processes. The possibility that every bright galaxy harbors a central, massive black hole—a remnant of a prior active past—is a wild card in the stack of potentially important astrophysical input.

In spite of—or, for the suitably geared-up simulator, because of—the inherent complexity, the problem attracts attention, and will continue to do so because of the many important roles played by galaxies in astrophysics and cosmology. The current state of affairs is represented in Fig. 4. An image of the local spiral galaxy M100 taken by the refurbished Hubble Space Telescope is shown alongside one of the best attempts at making a local disk replica under realistic cosmological conditions. The lack of fine detail in the simulation is indicative of both inadequate numerical resolution (there are roughly 30,000 star particles in the simulated disk compared with 10^{10} stars in M100) and an incomplete physical description.

According to Sir Martin Rees, Astronomer Royal of Britain, the job of predicting where galaxies will form in a cosmological volume is similar to that of predicting the weather. Each is a type of "environmental" science, in which the objective is to understand the workings of a highly nonlinear dynamical system characterized by complex, uncertain chemical and thermodynamic processes. Perhaps there's reason for optimism in this analogy. The accuracy of 5-day forecasts has improved markedly over the past decade, fueled in part by improvements in modeling but mostly by better input from more advanced weather satellites. As increasingly sensitive and detailed observations of galaxy formation are revealed by 10-m class telescopes on the ground and next-generation observatories in space, we will find in these data the clues necessary to build better virtual galaxies.

Real or Virtual Large-Scale Structure?

The key to image pairs in the figures is as follows: Fig. 1, left panel is virtual, right is real; Fig. 2, upper is real, lower is virtual; Fig. 3, left is real, right is virtual; Fig. 4, upper is real, lower is virtual.

I am very grateful to colleagues who helped produce the images used in this article: S. Cole, P. Norberg, D. Weinberg, R. Davé, J. Mohr, B. Mathiesen, and M. Steinmetz. I also thank D. Weinberg and K. King-Evrard for useful discussions.

1. Ostriker, J. P. & Norman, M. L. (1997) *Commun. ACM* **40,** 85–94.
2. Guth, A. (1981) *Phys. Rev. D* **23,** 347–357.
3. Wright, E. L., Meyer, S. S., Bennett, C. L., Boggess, N. W., Cheng, E. S., Hauser, M. G., Lineweaver, A. C., Mather, J. C., Smoot, G. F., Weiss, R., *et al.* (1992) *Astrophys. J.* **396,** L13–L17.
4. Frenk, C. S., *et al.* (1999) *Astrophys. J.*, in press.
5. Peebles, P. J. E. (1980) *The Large-Scale Structure of the Universe* (Princeton Univ. Press, Princeton).
6. Geller, M. J. & Huchra, J. P. (1989) *Science* **246,** 897–899.
7. Cole, S., Hatton, S., Weinberg, D. H. & Frenk, C. S. (1998) *Mon. Not. R. Astron. Soc.* **300,** 945–957.
8. Bond, J. R., Kofman, L. & Pogosyan, D. (1996) *Nature* **380,** 603–604.
9. Loveday, J, Maddox, S. J., Efstathiou, G. & Peterson, B. A. (1995) *Astrophys. J.* **442,** 457–468.
10. Jenkins, A. and the Virgo Consortium (1998) *Astrophys. J.* **499,** 20–33.
11. Gunn, J. E. & Peterson, B. A. (1965) *Astrophys. J.* **142,** 1633–1644.
12. Cen, R., Miralda-Escudé, J., Ostriker, J. P. & Rauch, M. (1994) *Astrophys. J.* **437,** L9–L12.
13. Zhang, Y., Anninos, P. & Norman, M. L. (1995) *Astrophys. J.* **453,** L57–L60.
14. Hernquist L., Katz, N., Weinberg, D. H. & Miralda-Escudé, J. (1996) *Astrophys. J.* **457,** L5–L8.
15. Songaila, A. & Cowie, L. L. (1996) *Astron. J.* **112,** 335–348.
16. Weinberg, D. H., Miralda-Escudé, J., Hernquist, L. & Katz, N. (1997) *Astrophys. J.* **490,** 564–572.
17. Burles, S. & Tytler, D. (1998) *Astrophys. J.* **507,** 732–744.
18. Ostriker, J. P. (1998) *Bull. AAS* **192,** 31040 (abstr.).
19. Bi, H. G. & Davidsen, A. (1997) *Astrophys. J.* **479,** 523–536.
20. Hui, L., Gnedin, N. & Zhang, Y. (1997) *Astrophys. J.* **486,** 599–609.
21. Croft, R. A. C., Weinberg, D. H., Pettini, M., Katz, N. & Hernquist, L. (1999) *Astrophys. J.,* in press, astro-ph/9809401.
22. Zwicky, F. (1933) *Helv. Phys. Acta* **6,** 110–115.
23. Evrard, A. E. (1990) *Astrophys. J.* **363,** 349–366.
24. Mohr, J. J., Mathiesen, B. & Evrard, A. E. (1999) *Astrophys. J.,* in press (astro-ph/9901281).
25. Mohr, J. J. & Evrard, A. E. (1997) *Astrophys. J.* **491,** 38–44.
26. Arnaud, M. & Evrard, A. E. (1999) *Mon. Not. R. Astron. Soc.,* in press (astro-ph/9806353).
27. Evrard, A. E. (1997) *Mon. Not. R. Astron. Soc.* **292,** 289–297.
28. Kirshner, R. P. (1999) *Proc. Natl. Acad. Sci. USA* **96,** 4224–4227.
29. Steidel, C. (1999) *Proc. Natl. Acad. Sci. USA* **96,** 4232–4235.